AFRL-AFOSR-VA-TR-2024-0131

Quantum Enhanced Precision and Stability of Atomic Clocks

CHRISTOPHER GERRY
Research Foundation Of The City University Of New York
250 Bedford Park B
Bronx, NY, 10468-2524
US

01/26/2024
Final Technical Report

Air Force Research Laboratory
Air Force Office of Scientific Research
Arlington, Virginia 22203
Air Force Materiel Command

REPORT DOCUMENTATION PAGE

PLEASE DO NOT RETURN YOUR FORM TO THE ABOVE ORGANIZATION.

1. REPORT DATE	2. REPORT TYPE	3. DATES COVERED	
20240126	Final	START DATE 20180515	END DATE 20191114

4. TITLE AND SUBTITLE
Quantum Enhanced Precision and Stability of Atomic Clocks

5a. CONTRACT NUMBER	5b. GRANT NUMBER	5c. PROGRAM ELEMENT NUMBER
	FA9550-18-1-0318	61102F
5d. PROJECT NUMBER	**5e. TASK NUMBER**	**5f. WORK UNIT NUMBER**

6. AUTHOR(S)
Christopher Gerry

7. PERFORMING ORGANIZATION NAME(S) AND ADDRESS(ES)
Research Foundation Of The City University Of New York
250 Bedford Park B
Bronx, NY 10468-2524
US

8. PERFORMING ORGANIZATION REPORT NUMBER

9. SPONSORING/MONITORING AGENCY NAME(S) AND ADDRESS(ES)	10. SPONSOR/MONITOR'S ACRONYM(S)	11. SPONSOR/MONITOR'S REPORT NUMBER(S)
Air Force Office of Scientific Research 875 N. Randolph St. Room 3112 Arlington, VA 22203	AFRL/AFOSR RTB1	AFRL-AFOSR-VA-TR-2024-0131

12. DISTRIBUTION/AVAILABILITY STATEMENT
A Distribution Unlimited: PB Public Release

13. SUPPLEMENTARY NOTES

14. ABSTRACT
The goal of this work was to study theoretically the prospect of enhancing the precision and stability of atomic clocks though the use of collective effects in ensembles of atoms and through the use of alternatives to the usual observable, namely the population of the excited state of the atoms. We assumed that each atom possess only two relevant levels (such as the
two hyperfine levels of cesium-133) where the transitions between these levels are driven by resonant (or near resonant) classical coherent radiation fields. Lessons learned form our work in quantum optical interferometry were brought to bear on this work. Quantum optical interferometry is similar to Ramsey spectroscopy, also known at population spectroscopy. In
the present work we considered the Ramsey method with collections of unetangled atoms where the monitored observable was the probability that all the atoms are in their excited states at the end of the Ramsey sequence of pulses and free evolution. We found that this technique narrows the central Ramsey fringe due to collective effects. It is the narrowing of
the central fringe that can result in enhanced precision and stability. We also studied cases where the atoms are entangled, but we discovered that a different observable must be use, namely the atomic parity, this being -1 raised to the number of atoms in the excited state.

15. SUBJECT TERMS

16. SECURITY CLASSIFICATION OF:			17. LIMITATION OF ABSTRACT	18. NUMBER OF PAGES
a. REPORT U	b. ABSTRACT U	c. THIS PAGE U	UU	21

19a. NAME OF RESPONSIBLE PERSON	19b. PHONE NUMBER *(Include area code)*
GRACE METCALFE	(703) 696-9740

Standard Form 298 (Rev.5/2020)
Prescribed by ANSI Std. Z39.18

Measurement Resolution in Multi-Atom Atomic Clocks

Christopher C. Gerry and Richard J. Birrittella Jr.

August 17, 2020

Abstract

The goal of this work rests primarily towards enhancing measurement resolution in atomic spectroscopy for frequency standards where our principal focus lies in quantum-enhanced improvement of atomic clock precision and stability. For atomic frequency standards, the transition frequency serves as a reliable 'master pendulum' whose oscillations mark the passage of time. This is because this transition frequency is incredibly stable. In general radiation is not precisely at resonant frequency, but instead is spread over a frequency range $\Delta\omega$. The precision to which the resonant frequency can be measured is proportional to the quality factor $Q = \omega_0/\Delta\omega$, where larger Q signifies a more stable atomic clock. Enhancing measurement resolution would lead to a smaller frequency uncertainty and thus result in a more accurate and stable atomic clock. In this work we consider two means of achieving this: first, we consider the use of multi-atom ensembles over the usual single-atom input. In our studies, we consider both the readily available unentangled atomic coherent state (ACS) as well as the entangled and spin-squeezed $\hat{J}_z$-operated ACS. We find that for the same selection of detection observables, the spin-squeezed state yields greater measurement resolution over the ACS which in turn yields greater resolution over the usual means of using a single-atom input. Second, we consider the use of detection observables that have no classical analog. To this end, we introduce the atomic analog of the parity operator, which in the context of quantum optical interferometry is known to saturate the quantum Cramer-Raó bound, making it the optimal detection observable to minimize phase uncertainty. We go on to show that for any input state, atomic parity yields the greatest measurement resolution.

Contents

Introduction

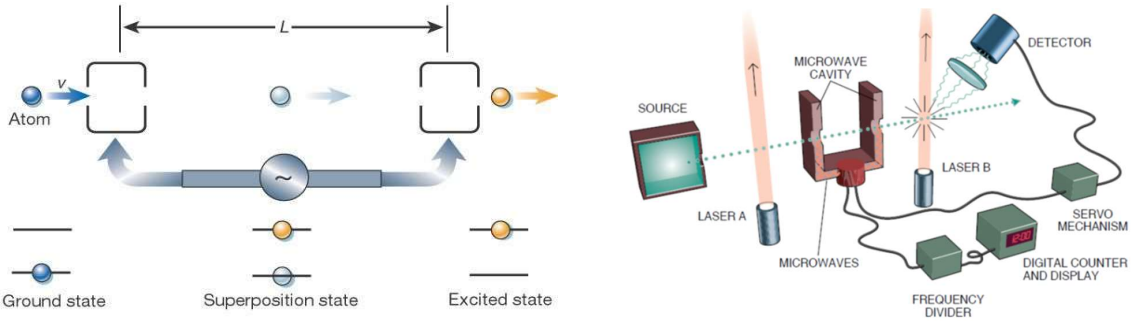

Figure 1: Ramsey method of separated fields for a single two-level atom.(left) A schematic tracking the atomic state through each operation. (right) a diagram detailing the experimental procedure. Figures taken from: Itano and Ramsey *Scientific American* **269** 1 (1993) pp. 56-65.

We consider the Ramsey spectroscopy technique of separated oscillatory fields with ensembles of two-level atoms but with new detection schemes that yield much more highly resolved Ramsey fringes than is possible in the usual implementation of the Ramsey technique; we were interested in producing Ramsey fringes that are much narrower than those normally obtained. The usual approach in atomic frequency standards, see Fig. 1 is to consider the use of a single two-level atom, initially prepared in its ground state. The first $\pi/2$-pulse, performed via optical pumping, places the atom in a superposition state of its two internal degrees of freedom. Afterwards, the atom undergoes a period of free evolution, resulting in a phase shift of $\phi = (\omega - \omega_0)T$ where ω, ω_0, and T correspond to the resonant frequency of the two energy levels, the frequency of the radiation and free evolution time, respectively. The final $\pi/2$ pulse, if the resulting radiation is on resonance, will result in the atom being found in its excited state with a probability $P_{\text{Excited}} = 1$. See Figure 2 for a Bloch sphere representation of the process.

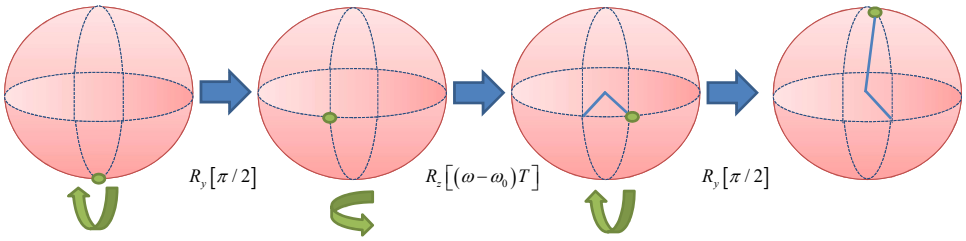

Figure 2: Bloch sphere representation for single-atom spectroscopy. The atom is intially in its ground state. The first $\pi/2$-pulse places the atom in a superposition state while the free evolution corresponds to a rotation in the $x - y$ plane. The final $\pi/2$-pulse, if on resonance, places the atom in the excited state. For a frequency-spread in radiation $\Delta\omega$ the state will be nearly at the north pole of the Bloch sphere.

In what follows, we present our work in the area of atomic interferometry where each atom is assumed to possess only two relevant energy levels (degrees of freedom), ground and excited, and where transitions between these levels are driven by classical coherent radiation fields (or microwave fields in the case of trapped ions). Of specific interest is the use of atomic parity, defined with respect to the excited state, as a detection observable. This can be expressed both in terms of the boson operators $\{\hat{a}^\dagger, \hat{b}^\dagger\}$, which creates an atom in the excited and ground state, respectively, as well as the Schwinger realization of the SU(2) algebra as $\hat{\Pi} = (-1)^{\hat{a}^\dagger \hat{a}} = (-1)^{\hat{J}_0 - \hat{J}_3}$, where $\hat{J}_{0(3)} = \frac{1}{2}(\hat{a}^\dagger \hat{a} \pm \hat{b}^\dagger \hat{b})$. This detection observable has no classical analog; it is a purely quantum mechanical construct.

It is worth discussing the underlying SU(2) alegbra involved in the representation of multi-atom atomic states and how the relevant parity operators (be it with respect to excited- or ground state occupation)

are defined in terms of the SU(2) operators. We begin with the definitions of the Dicke operators for a collection of N-atoms according to

$$\hat{J}_3 = \frac{1}{2}\sum_{i=1}^{N}\left(|e\rangle_i\langle e| - |g\rangle_i\langle g|\right) = \frac{1}{2}\sum_{i=1}^{N}\sigma_3^{(i)} \tag{1}$$

$$\hat{J}_+ = \sum_{i=1}^{N}|e\rangle_i\langle g| = \sum_{i=1}^{N}\sigma_+^{(i)} \tag{2}$$

$$\hat{J}_- = \sum_{i=1}^{N}|g\rangle_i\langle e| = \sum_{i=1}^{N}\sigma_-^{(i)} \tag{3}$$

$$\hat{J}_0 = \frac{1}{2}\sum_{i=1}^{N}\left(|e\rangle_i\langle e| + |g\rangle_i\langle g|\right) = \frac{1}{2}\sum_{i=1}^{N}\mathbf{I}^{(i)}, \tag{4}$$

where these operators satisfy the usual angular momentum, or SU(2), algebra and where $\hat{J}_0$ commutes with all the other operators. We can define the atomic parity operator as

$$\hat{\Pi}_e = (-1)^{\hat{J}_0+\hat{J}_3} = \exp\left[i\pi\left(\hat{J}_0+\hat{J}_3\right)\right]. \tag{5}$$

For a Dicke state $|j,m\rangle$, where $j = N/2$, we have

$$\hat{\Pi}_e|j,m\rangle = (-1)^{j+m}|j,m\rangle, \tag{6}$$

where $j+m$ is an integer and where

$$\hat{J}_0+\hat{J}_3 = \sum_{i=1}^{N}|e\rangle_i\langle e| \equiv N_e, \tag{7}$$

which represents the number of atoms in their excited states. That is, for a Dicke state $|j,m\rangle$, $j+m$ is the number of atoms in the excited state. Thus, we can define $\langle\hat{\Pi}_e\rangle = (-1)^{N_e}$. It is also worth pointing out that this detection observable can be defined with respect to the ground state population, that is, $\langle\hat{\Pi}_G\rangle = (-1)^{N_G}$. That is, we define parity with respect to the number of atoms found in their *ground* state. The two are related by $\langle\hat{\Pi}_{\text{Excited}}\rangle = (-1)^{2j}\langle\hat{\Pi}_{\text{Ground}}\rangle$.

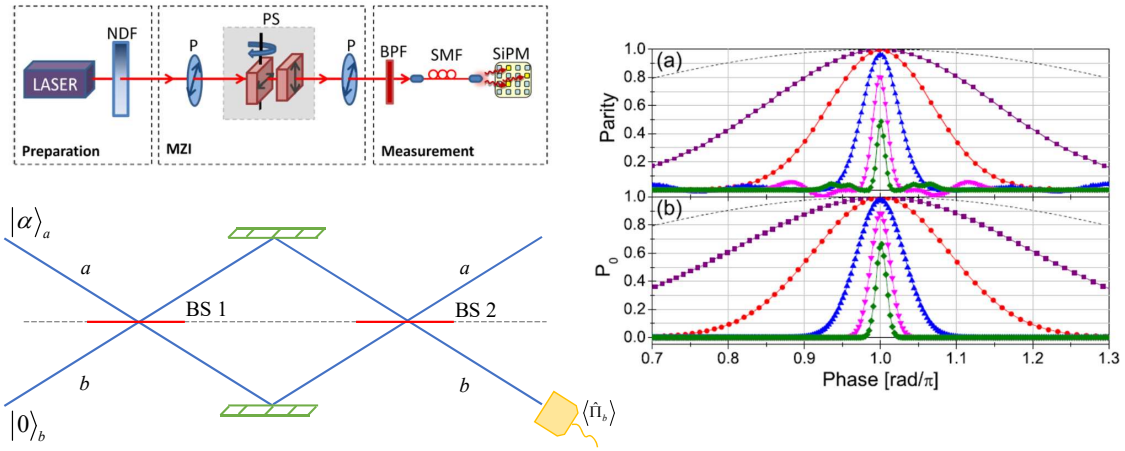

Figure 3: Use of optical parity as a detection observable employed experimentally for classical light in Cohen *et al.* (2014) **22** 10 along with a schematic of the set-up used as well as the expectation value of the parity operator. Note that the narrowing of the peak corresponds to an enhancement in measurement resolution.

There is some precedent in the use of parity as a detection observable in the optical case. In the context of quantum optical interferometry, parity has been shown to enhance measurement resolution as well as being the optimal detection observable which saturates the quantum Cramer-Raó bound, maximizing the quantum Fisher information. For the case of input coherent light mixed with a vacuum inside a Mach-Zehnder interferometer (MZI), parity has been successfully experimentally employed in measurements

of the phase uncertainty $\Delta\phi$, yielding the well known limit for classical light: the standard quantum limit (or shot-noise limit). A schematic of the experimental set-up and measurement resolution, taken from Cohen *et al.* **22** 10 (2014), is given in Fig. 3. As motivation, we will begin by detailing the most extreme of ideal cases: using atomic parity as a detection observable while having the state after the first$\pi/2$-pulse be an atomic N00N state.

1 Ideal Case – Parity-based resolution for an initial atomic N00N state

To aid in motivating the subject of this work, we first consider the most ideal of cases, that is, we analyze the measurement resolution obtained in a Ramsey interferometer using parity-based detection, where the state after the first $\pi/2$-pulse is the atomic N00N state, given by

$$|\psi\rangle_{\mathrm{N00N}} = \frac{1}{\sqrt{2}}\left(|j,j\rangle + e^{i\lambda}\,|j,-j\rangle\right), \tag{8}$$

where the Dicke states $|j,m\rangle$, are defined in terms of the individual atomic states as $|j,j\rangle = |\mathrm{e}\rangle^{\otimes N=2j}$ and $|j,-j\rangle = |\mathrm{g}\rangle^{\otimes N=2j}$ with intermediate steps consisting of superpositions of all permutations with consecutively more atoms being found in the ground state all the way down to $|j,-j\rangle$, where all atoms are in the ground state. With this in mind, the state given in Eq. 8 is simply a superposition of all atoms found in the ground- or all atoms found in the excited- state. This can be expressed as a finite sum over all Dicke states as

$$|\psi\rangle_{\mathrm{N00N}} = \sum_{m=-j}^{j} \Lambda_m^{(j)}\,|j,m\rangle\,, \tag{9}$$

where the coefficients $\Lambda_m^{(j)}$ are given by

$$\Lambda_m^{(j)} = \frac{1}{\sqrt{2}}\left(\delta_{m,j} + e^{i\lambda}\delta_{m,-j}\right). \tag{10}$$

This state is of interest as it is the atomic analog of the optical N00N state $|\psi\rangle_{\mathrm{N00N}} = \frac{1}{\sqrt{2}}\big(\,|N,0\rangle + e^{i\lambda}\,|0,N\rangle\,\big)$, which yields the lower bound on phase uncertainty in quantum optical interferometry: the Heisenberg limit. This follows from the heuristic uncertainty relation between photon number and phase $\Delta\phi\Delta N \simeq 1$, where the N00N state maximizes the uncertainty in photon number, that is, $\Delta N = N \;\rightarrow\; \Delta\phi \simeq 1/\Delta N = 1/N$. The action of the interferometer is once again given by

$$|\Psi_{\mathrm{F}}\rangle = e^{-i\frac{\pi}{2}\hat{J}_y} e^{-i\phi\hat{J}_z}\,|\psi\rangle_{\mathrm{N00N}}\,, \tag{11}$$

where we assume some means of experimentally generating the atomic N00N state is employed prior to free evolution. Here we introduce the atomic parity operator as $\hat{\Pi} = \mathrm{Exp}\big[i\pi\big(\hat{J}_0 + \hat{J}_3\big)\big]$, with respect to the number of atoms found in the excited state. This is simply (-1) raised to the number of atoms in the excited state. We can likewise define atomic parity in terms of the number of atoms found in the ground state. The relationship between the two being $\langle\hat{\Pi}_{\mathrm{Ground}}\rangle = (-1)^{2j}\,\langle\hat{\Pi}_{\mathrm{Excited}}\rangle$. This is sensible, since if N is even and $2n$ atoms are excited then $2n'$ atoms must also be in the ground state where $n, n' \in \mathbb{Z}^+$. A similar argument can be made for $2n+1$ exicted atoms. Likewise, if N were odd and $2n$ atoms are excited, then $2n'+1$ must be in the ground state, resulting in a sign difference in parity. With this, we can derive an expression for the expectation value of the parity operator for the state given by Eq. 11 using the identity in Eq. 28 to find

$$\begin{aligned}\langle\hat{\Pi}\rangle_{\mathrm{N00N}} &= (-1)^{2j}\sum_{m=-j}^{j}\Lambda_m^{(j)}\Lambda_{-m}^{(j)*}e^{-i2\phi m}\\ &= (-1)^N\cos N\phi,\end{aligned} \tag{12}$$

where $N = 2j$, the total number of atoms. Note the fact the expression in Eq. 12 does not depend on the phase λ defined in Eq. 8. Once again we see a narrowing of the peak centered at the origin for increasing numbers of atoms N. This results in finer measurement resolution and ultimately enhanced phase sensitivity in interferometric measurements. This state would serve as the ideal, as it is maximally entangled and yields the greatest measurement resolution for a given detection observable. The problem,

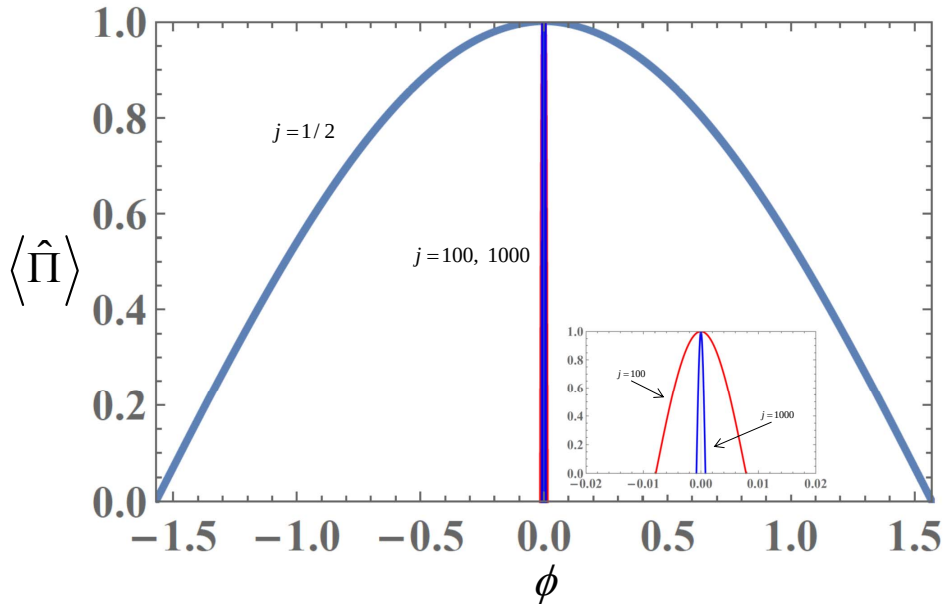

Figure 4: Parity-based resolution with a resultant atomic N00N state after the first $\pi/2$-pulse in a Ramsey interferometer for $j = 1/2,\ 100,\ 1000$.

however, is atomic N00N states are incredibly difficult to make. We endeavor to find means of enhancing measurement resolution by considering different detection observables as well as states that are readily available experimentally.

2 Resolution using $\langle \hat{J}_z \rangle$ as a detection observable

Consider a general atomic state expressed in terms of a superposition of all Dicke states $|j, m\rangle$, where the Dicke states are defined relative to the individual atomic states in the previous section, given by

$$|\psi'\rangle = \sum_{m=-j}^{j} C_m^{(j)} |j, m\rangle \,. \tag{13}$$

Let Eq. 13 describe the state *after* the first $\pi/2$-pulse in a Ramsey interferometer, where $C_m^{(j)}$ are the probability amplitudes for obtaining the each $|j, m\rangle$. The state after the time evolution and the final $\pi/2$-pulse is given by

$$\begin{aligned} |\Psi\rangle &= e^{-i\frac{\pi}{2}\hat{J}_y} e^{-i\phi\hat{J}_z} |\psi'\rangle \\ &= \sum_{m'=-j}^{j} \left[\sum_{m=-j}^{j} C_m^{(j)} e^{-i\phi m} d^j_{m',m}\left(\tfrac{\pi}{2}\right) \right] |j, m'\rangle \\ &= \sum_{m'=-j}^{j} \tilde{C}_{m'}^{(j)} |j, m'\rangle \,, \end{aligned} \tag{14}$$

where $\tilde{C}_{m'}^{(j)}$ are defined within the square brackets of Eq. 14 and $d^j_{m',m}(\beta)$ are the usual Wigner-d matrix elements given by $\langle j, m'|e^{-i\beta\hat{J}_y}|j, m\rangle$. We consider the measurement resolution obtained for this general case when using $\langle \hat{J}_z \rangle$ as our detection observable. Physically, this corresponds to taking the difference between the number of atoms in the ground and excited states, respectively. The optical analog would be taking the difference in intensity between the two output modes of an MZI. The expectation value of $\hat{J}_z$ is given by

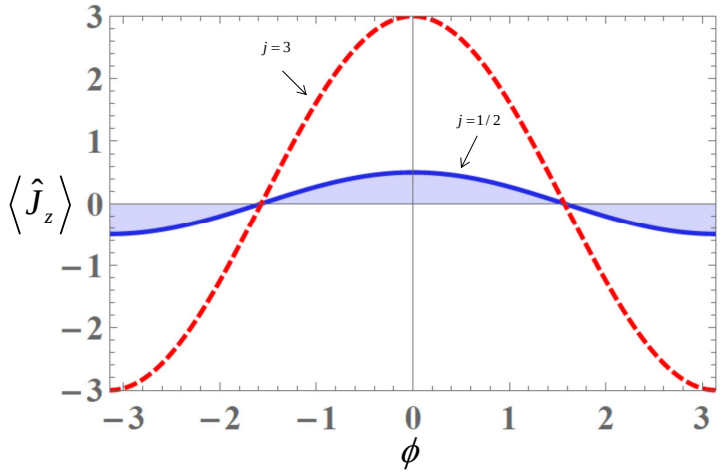

Figure 5: $\langle \hat{J}_z \rangle$ versus ϕ for a couple of j values. Note that we do not see a change in resolution for larger numbers of atoms.

$$\begin{aligned}\langle \hat{J}_z \rangle &= \sum_{m=-j}^{j} \sum_{p=-j}^{j} C_p^{(j)*} C_m^{(j)} e^{i\phi(m-p)} \times \left[\sum_{m'=-j}^{j} m' d^j_{m',p}\left(\tfrac{\pi}{2}\right) d^j_{m',m}\left(\tfrac{\pi}{2}\right) \right] \\ &= \sum_{m=-j}^{j} \sum_{p=-j}^{j} C_p^{(j)*} C_m^{(j)} e^{i\phi(m-p)} \times \Gamma_{m,p}\left(\tfrac{\pi}{2}\right), \end{aligned} \tag{15}$$

where the function $\Gamma_{m,p}(\lambda)$ can be simplified to

$$\begin{aligned}\Gamma_{m,p}(\lambda) = \sum_{m'=-j}^{j} \Big(& m' d^j_{m',m}(\lambda)\, d^j_{m',m+1}(\lambda)\, \delta_{p,m+1} + \\ & + m' d^j_{m',p+1}(\lambda)\, d^j_{m',p}(\lambda)\, \delta_{p+1,m} + m' d^j_{m',p}(\lambda)\, d^j_{m',p}(\lambda)\, \delta_{p,m} \Big). \end{aligned} \tag{16}$$

Plugging this back into Eq. 15 and assuming, without loss of generality, the coefficients $C_m^{(j)}$ are real, we obtain the result

$$\langle \hat{J}_z \rangle = \gamma^{(j)} \cos\phi + \alpha^{(j)}, \tag{17}$$

where

$$\gamma^{(j)} = 2 \sum_{m=-j}^{j} \sum_{m'=-j}^{j} C_m^{(j)} C_{m+1}^{(j)} d^j_{m',m}\left(\tfrac{\pi}{2}\right) d^j_{m',m+1}\left(\tfrac{\pi}{2}\right) m' \tag{18}$$

$$\alpha^{(j)} = \sum_{m=-j}^{j} \sum_{m'=-j}^{j} \left| C_m^{(j)} d^j_{m,m'}\left(\tfrac{\pi}{2}\right) \right|^2 m'. \tag{19}$$

For the limiting case of the atomic coherent state, this yields the well known result

$$\langle \hat{J}_z \rangle_{\mathrm{ACS}} = j \cos\phi, \tag{20}$$

which we plot in Fig. 5 for several values of j. Similarly, by playing the same game for $\langle \hat{J}_z^2 \rangle$, we obtain the result

$$\langle \hat{J}_z^2 \rangle = \Omega^{(j)} \cos 2\phi + \kappa^{(j)}, \tag{21}$$

where

$$\Omega^{(j)} = 2\sum_{m=-j}^{j}\sum_{m'=-j}^{j} C_{m+2}^{(j)} C_{m}^{(j)} m'^{2} d^{j}_{m',m+2}\left(\tfrac{\pi}{2}\right) d^{(j)}_{m',m}\left(\tfrac{\pi}{2}\right) \tag{22}$$

$$\kappa^{(j)} = \sum_{m=-j}^{j}\sum_{m'=-j}^{j}\left| C_{m}^{(j)} d^{j}_{m',m}\left(\tfrac{\pi}{2}\right) m'\right|^{2}. \tag{23}$$

Note that in neither case do we see a narrowing of the peak regardless of the state used. The phase dependency goes as a cosine function regardless of the state coefficients and number of atoms used. This particular detection observable cannot yield enhanced measurement resolution regardless of the initial state under consideration.

3 Resolution using $\langle\hat{\Pi}\rangle$ as a detection observable

Let us assume our state is initially prepared with all atoms in the ground state, that is $|\text{in}\rangle = |j,-j\rangle$. The action of the Ramsey interferometer is to transform an initial state $|\psi'\rangle$ by

$$\begin{aligned} |\Psi_{\text{F}}\rangle &= e^{-i\frac{\pi}{2}\hat{J}_y} e^{-i\phi\hat{J}_z} e^{-i\frac{\pi}{2}\hat{J}_y} |\psi'\rangle \\ &= e^{-i\frac{\pi}{2}\hat{J}_y} e^{-i\phi\hat{J}_z} |\zeta=-1,j\rangle\,, \end{aligned} \tag{24}$$

where the state $|\zeta=-1,j\rangle$ is an atomic coherent state in which all of atoms are in the superposition state $\frac{1}{\sqrt{2}}\big(|e\rangle - |g\rangle\big)$, that is,

$$|\zeta=-1,j\rangle = \frac{1}{2^{N/2}}\left(|\text{e}\rangle - |\text{g}\rangle\right)^{\otimes N=2j} \;=\; 2^{-j}\sum_{m=-j}^{j}\binom{2j}{j+m}^{1/2}(-1)^{j+m}\,|j,m\rangle\,, \tag{25}$$

where in the last term we express the state in terms of the Dicke states. Let us recover the known result for parity-based detection for an atomic coherent state. The final state after the interferometer is

$$|\Psi_{\text{F}}\rangle = 2^{-j}\sum_{m=-j}^{j}\sum_{m'=-j}^{j}\binom{2j}{j+m}^{1/2}(-1)^{j+m}\,e^{-i\phi m} d^{j}_{m',m}\left(\tfrac{\pi}{2}\right)|j,m'\rangle\,, \tag{26}$$

and the expectation value of the parity operator can be expressed as

$$\begin{aligned} \langle\hat{\Pi}\rangle = 2^{-2j}\sum_{m=-j}^{j}\sum_{p=-j}^{j}&\binom{2j}{j+m}^{1/2}\binom{2j}{j+p}^{1/2} e^{i\pi(2j+m+p)} e^{-i\phi(m-p)}\times \\ &\times\left[\sum_{m'=-j}^{j}(-1)^{j-m'} d^{j}_{m',m}\left(\tfrac{\pi}{2}\right) d^{j}_{m',p}\left(\tfrac{\pi}{2}\right)\right], \end{aligned} \tag{27}$$

where the atomic parity operator $\hat{\Pi}$ is defined explicitly in the previous section. The term in the square brackets, expressed below as $F_{m,p}(\lambda)$, can be simplified to

$$\begin{aligned} F_{m,p}(\lambda) &= \sum_{m'=-j}^{j}(-1)^{j-m'} d^{j}_{m',m}(\lambda)\, d^{j}_{m',p}(\lambda) \\ &= (-1)^{2j}\sum_{m'} d^{j}_{m',-m}(\pi-\lambda)\, d^{j}_{m',p}(\lambda) \\ &= (-1)^{2j}\sum_{m'} d^{j}_{p,m'}(-\lambda)\, d^{j}_{m',-m}(\pi-\lambda) \\ &= (-1)^{2j} d^{j}_{p,-m}(\pi-2\lambda)\,. \end{aligned} \tag{28}$$

Plugging this back into Eq. 27, noting $F_{m,p}\left(\lambda\to\frac{\pi}{2}\right) = (-1)^{2j}\,\delta_{-m,p}$, we find

$$\langle\hat{\Pi}\rangle = 4^{-j}\sum_{m=-j}^{j}\binom{2j}{j+m} e^{-i2\phi m}(-1)^{4j} = d^{j}_{-j,-j}(2\phi) = \cos^{2j}\phi, \tag{29}$$

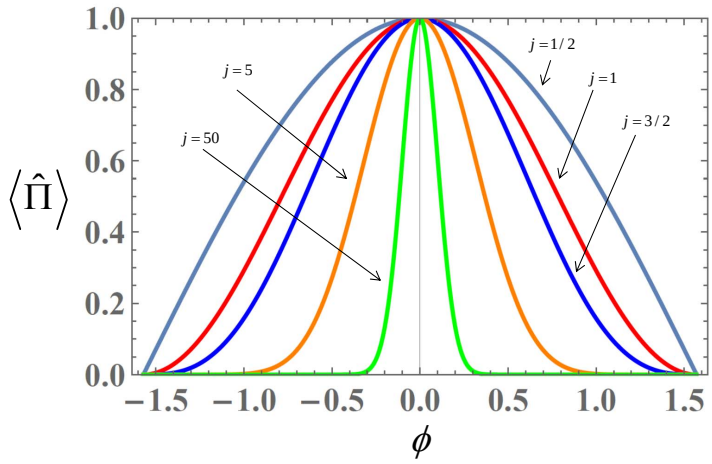

Figure 6: Expectation value of the parity operator for an initial atomic coherent state. Note the increased resolution as the number of atoms is increased.

which is the known result, plotted in Fig. 6. Note that we see an increase in measurement resolution as the number of atoms increases. Let's consider the case where we act with the $\hat{J}_z$ operator after the first $\pi/2$-pulse. The resulting state is both entangled on the atomic-state level and displays a quality known as spin-squeezing which has been shown to reduce projection noise in high-precision population spectroscopy. In this case the initial state is transformed by

$$\begin{aligned} |\Psi_{\mathrm{F}}\rangle &= e^{-i\frac{\pi}{2}\hat{J}_y} e^{-i\phi\hat{J}_z} \hat{J}_z e^{-i\frac{\pi}{2}\hat{J}_y} |\mathrm{in}\rangle \\ &= e^{-i\frac{\pi}{2}\hat{J}_y} e^{-i\phi\hat{J}_z} |\zeta = -1, j; 1\rangle , \end{aligned} \tag{30}$$

where the state

$$\begin{aligned} |\zeta = -1, j; 1\rangle &\propto \hat{J}_z |\zeta = -1, j\rangle \\ &= \left(2^{2j-1} j\right)^{-1/2} \sum_{m=-j}^{j} \binom{2j}{j+m}^{1/2} (-1)^{j+m} m |j, m\rangle . \end{aligned} \tag{31}$$

Once again, we use Eq. 28 to find the expectation value of the parity operator

$$\begin{aligned} \langle \hat{\Pi} \rangle &= -\left(2^{2j-1} j\right)^{-1} \sum_{m=-j}^{j} \binom{2j}{j+m} m^2 e^{-i2\phi m} \\ &= -\frac{2}{\pi} \frac{\Gamma\left(j+\frac{1}{2}\right)}{\Gamma\left(j+2\right)} e^{-i2\phi} \left[{}_3F_2\left(2, 2, 1-j; 1, j+2; -e^{-i2\phi}\right) + e^{i4\phi} {}_3F_2\left(2, 2, 1-j; 1, j+2; -e^{i2\phi}\right) \right], \end{aligned} \tag{32}$$

where ${}_3F_2$ is the hypergeometric function given by

$${}_pF_q\left(a_1, ..., a_p; b_1, ..., b_q; z\right) = \sum_{n=0}^{\infty} \frac{(a_1)_n \ldots (a_p)_n}{(b_1)_n \ldots (b_q)_n} \frac{z^n}{n!}, \tag{33}$$

where we use the Pochhammer symbol to express $(x)_n = x\,(x+1)\,(x+2)\ldots(x+n-1)$ for $n \geq 1$. For several different values of j, we use Eq. 32 to find

$$
\begin{aligned}
j = 1/2 \quad &\rightarrow \quad \langle \hat{\Pi} \rangle = -\cos\phi \\
j = 1 \quad &\rightarrow \quad \langle \hat{\Pi} \rangle = -\cos 2\phi \\
j = 3/2 \quad &\rightarrow \quad \langle \hat{\Pi} \rangle = -\tfrac{1}{2}\cos\phi\,(3\cos 2\phi - 1) \\
j = 2 \quad &\rightarrow \quad \langle \hat{\Pi} \rangle = -\cos^2\phi\,(2\cos 2\phi - 1) \\
j = 5/2 \quad &\rightarrow \quad \langle \hat{\Pi} \rangle = -\tfrac{1}{2}\cos^3\phi\,(5\cos 2\phi - 3) \\
j = 3 \quad &\rightarrow \quad \langle \hat{\Pi} \rangle = -\cos^4\phi\,(3\cos 2\phi - 2) \\
j = 7/2 \quad &\rightarrow \quad \langle \hat{\Pi} \rangle = -\tfrac{1}{2}\cos^5\phi\,(7\cos 2\phi - 5) \\
j = 4 \quad &\rightarrow \quad \langle \hat{\Pi} \rangle = -\cos^6\phi\,(4\cos 2\phi - 3)\,.
\end{aligned}
\tag{34}
$$

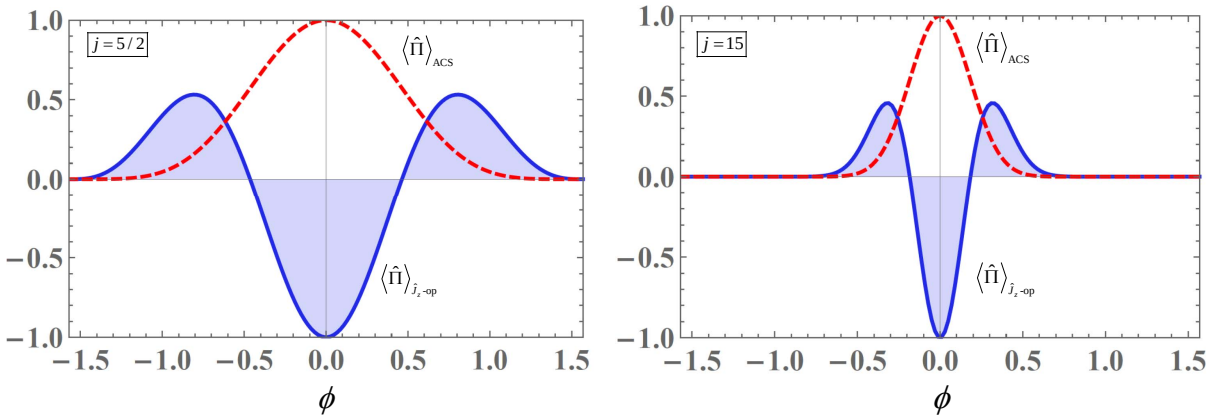

(a) (b)

Figure 7: Resolution obtained via parity-based detection for the $\hat{J}_z$-operated atomic coherent state and the atomic coherent state for: (a) $j = 5/2$ and (b) $j = 15$. Note that in each case, the resolution obtained via the $\hat{J}_z$-operated atomic coherent state exceeds the resolution obtained via the atomic coherent state for the same value of j..

So we see that the presence of spin-squeezing, in this case the $\hat{J}_z$-operated atomic coherent state, we get greater resolution with increasing increasing number of atoms. This yields an improvement of measurement resolution over the standard unentangled atomic coherent states.

4 Resolution using Ground/Excited state detection

Another detection observable that displays greater resolution for increasing numbers of atoms is the ground-state projection operator $\hat{P}^{(j)}_{-j} = |j,-j\rangle\langle j,-j|$. This operator is the atomic analogue to the optical 'no-photon detection' measurement, which was proven to be a useful post-selection technique for enhancing phase sensitivity in quantum optical interferometry. Starting from the output state of the Ramsey interferometer, given by Eq. 30, the expectation value of the ground state projection operator is

$$
\langle \hat{P}^{(j)}_{-j} \rangle_{\mathrm{ACS}} = \left| 2^{-j} \sum_{m=-j}^{j} \binom{2j}{j+m}^{1/2} (-1)^{j+m}\, e^{-i\phi m} d^{j}_{-j,m}\left(\tfrac{\pi}{2}\right) \right|^2 . \tag{35}
$$

In Fig.(8), we compare the resolution obtained by way ground-state detection and parity-based detection. In both cases we see enhanced resolution for increasing j, though parity-based detection outperforms ground-state detection.

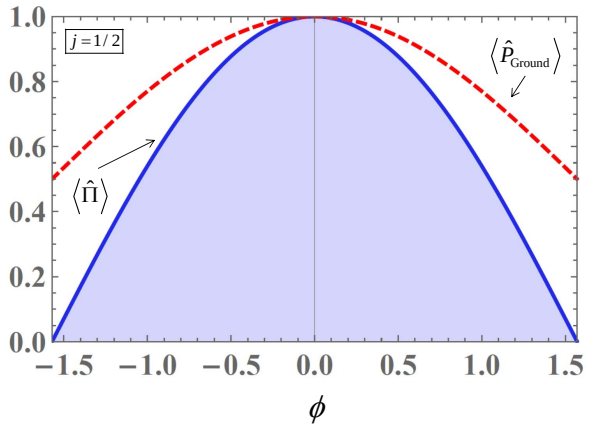

(a)

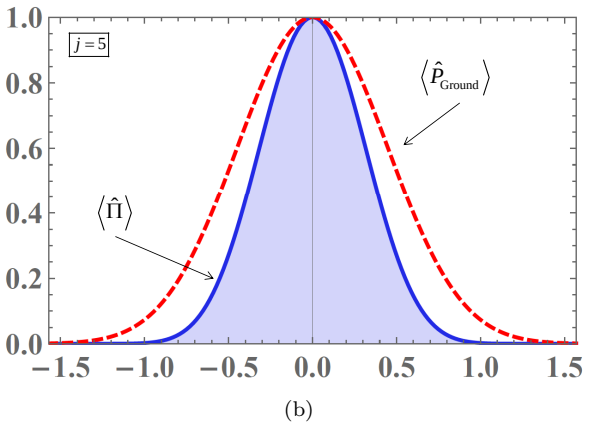

(b)

Figure 8: Ground state detection versus parity-based detection for: (a) $j = 1/2$ and (b) $j = 5$. Note that in each case, the resolution is enhanced for increasing j.

We can also explore the use of ground-state detection when we have an initial spin-squeezed state such as the $\hat{J}_z$-operated atomic coherent state. In this case, the expectation value of the ground-state projection operator is given by

$$\langle \hat{P}^{(j)}_{-j} \rangle_{\hat{J}_z\text{-op}} = \left| \left(2^{2j-1} j\right)^{-1/2} \sum_{m=-j}^{j} \binom{2j}{j+m}^{1/2} (-1)^{j+m} m e^{-i\phi m} d^{j}_{-j,m}\left(\tfrac{\pi}{2}\right) \right|^2 . \tag{36}$$

We plot a comparison of the resolution obtained via ground-state detection and parity-based detection in Fig.(9) for $j = 15$. Once again we see enhanced resolution for larger numbers of atoms. An important note should be made here: rather than projecting onto the state in which all atoms are found in the ground state, we can project onto the state in which all atoms are found in the excited state. This corresponds to the projection operator $P^{(j)}_{j} = |j, j\rangle \langle j, j|$ and the expectation value of this projection operator is related to the expectation value of the ground state projection operator by $P_{\mathrm{E}}(\phi) = P_{\mathrm{G}}(\phi \pm \pi)$ where

$$\langle P^{(j)}_{j} \rangle = P_{\mathrm{E}}(\phi), \qquad \langle P^{(j)}_{-j} \rangle = P_{\mathrm{G}}(\phi). \tag{37}$$

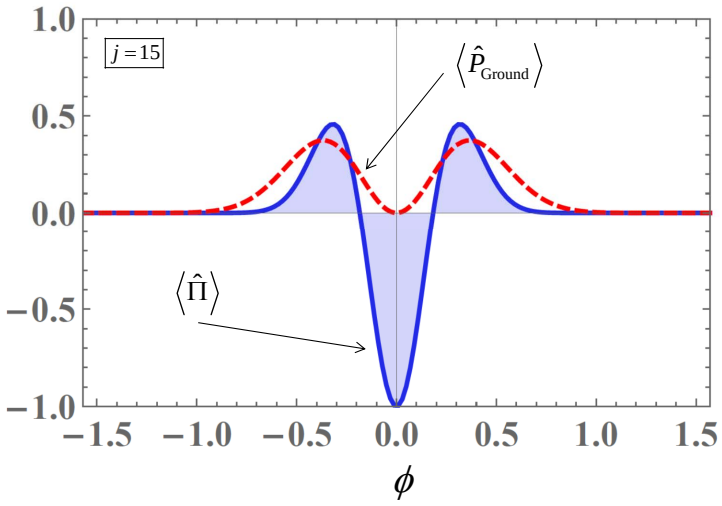

Figure 9: Ground state detection versus parity-based detection for an initial $\hat{J}_z$-operated atomic coherent state for $j = 15$.

5 A comparison of detection observables

Here we consider several of the 'detection observables' discussed previously. For a given number of atoms corresponding to $j = N/2 = 15$, we plot the following:

$\langle \hat{\Pi} \rangle$ = Expectation value of the parity operator,

$\langle \hat{\Pi}_{\text{Even}} \rangle$ = Probability of finding an even number of atoms in the excited state,

$\langle \hat{\Pi}_{\text{Odd}} \rangle$ = Probability of finding an odd number of atoms in the excited state,

$P_{\text{E}}(\phi) = \langle P_j^{(j)} \rangle$ = Probability of detecting all atoms in the excited state, (38)

$P_{\text{G}}(\phi) = \langle P_{-j}^{(j)} \rangle$ = Probability of detecting all atoms in the ground state,

$\langle \hat{J}_z \rangle / 2j$ = Scaled difference between number of atoms in excited and ground states,

$W_{\text{Inversion}} = P_{\text{E}}(\phi) - P_{\text{G}}(\phi)$ = Difference between probability of finding all atoms in excited and ground states.

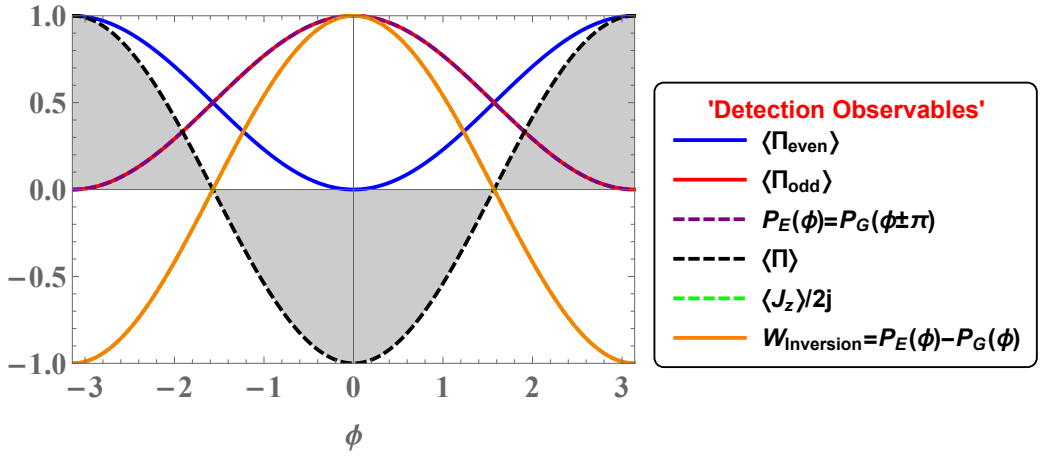

(a)

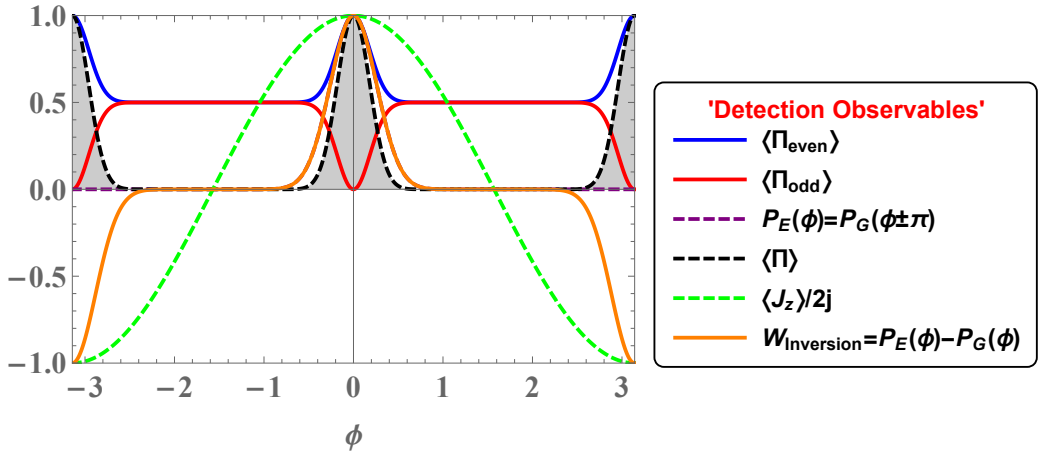

(b)

Figure 10: Measurement resolution for each detection observable for (a) $N = 2j = 1$ and (b) $N = 2j = 30$.

A plot for detailing the measurement resolution for each observable is given in Fig. 10 for several values of j (note: for the $j = 15$ case, the purple curve line follows the orange curve, except staying zero when the orange curve dips to -1). All measures except $\langle \hat{J}_z \rangle / 2j$ narrow with increasing numbers of atoms, however nothing gets as narrow as the expectation value of the parity operator $\langle \hat{\Pi} \rangle$. The only remaining question is: what does the expectation value of the parity operator mean exactly, in this context?

6 Projection onto the 'half atoms excited' state

Next we consider projection onto the 'half atoms excited and half atoms ground' state. This corresponds to projection onto the $|j, 0\rangle$ state, that is we define

$$P_M^{(j)} = |j, M\rangle \langle j, M| \quad \rightarrow \quad P_M(\phi) = \langle P_M^{(j)} \rangle , \tag{39}$$

which are simply the projection onto an arbitrary atomic state and corresponding probability of obtaining said state, respectively. Obviously in order for this to be well defined, an even number of atoms must be present. This corresponds to integer values of j. For $M = j$, we project onto the state in which all atoms are in the excited state and $M = -j$ all atoms in the ground state. These have been discussed in early sections. The case of immediate interest is projection onto the state in which half the atoms are in the excited state and half the atoms are in the ground state. This corresponds to $M = 0$ for integer values of j.

In Fig. 11 we plot several expectation values, including that of projection onto the $|j, j\rangle$ (all atoms excited) state, $|j, 0\rangle$ (half atoms excited, half ground) state, and parity for reference. Note that a $\pi/2$-

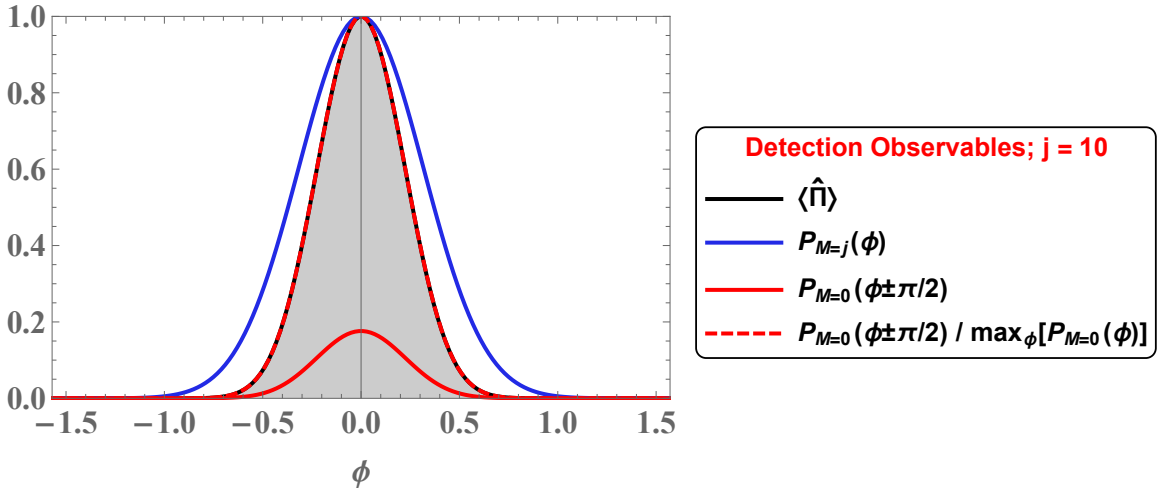

Figure 11: A plot of measurement resolution versus phase ϕ for projection onto several different atomic states.

phase shift is included for the projection onto the $|j,0\rangle$ state to place the peak at $\phi = 0$. Included in Fig. 11 is a scaled projection onto the $|j,0\rangle$ state, that is we plot

$$P_{M=0}\left(\phi \pm \pi/2\right) / \max_{\phi}\left[P_{M=0}\left(\phi\right)\right], \tag{40}$$

which is simply the probability of obtaining the $|j,0\rangle$ scaled to peak at one. A few things of note: first, for increasing values of j, the max probability of detecting the $|j,0\rangle$ state decreases. For example, for $j = 30$, the maximum probability of obtaining this state is $\sim 10\%$. Secondly, there *does* seem to be an enhancement in measurement resolution for increasing j, that is, the peak narrows. Thirdly, and most interestingly, the scaled projection onto the $|j,0\rangle$ seems to agree perfectly with the expectation value of the parity operator, $\langle\hat{\Pi}\rangle$. This seems to only be true for the case of an atomic coherent state generated after the first $\pi/2$-pulse. This will not work for the case of the spin-squeezed atomic coherent state, $\hat{J}_z\,|-1,j\rangle$. In summary, for the atomic coherent state, we can write

$$\langle\hat{\Pi}\rangle_{\mathrm{ACS}} = \frac{P^{(\mathrm{ACS})}_{M=0}\left(\phi \pm \pi/2\right)}{\max_{\phi}\left[P^{(\mathrm{ACS})}_{M=0}\left(\phi\right)\right]} = \frac{P^{(\mathrm{ACS})}_{M=0}\left(\phi \pm \pi/2\right)}{P^{(\mathrm{ACS})}_{M=0}\left(\pm\pi/2\right)}. \tag{41}$$

It seems to be relevant as the usual means of measurement relies on the detection of the excited state. If the probabilities can be monitored, and the maximum probability of obtaining the $|j,0\rangle$ state can be concluded (perhaps through repeated trials), then this may provide a means of determining the expectation value of the parity operator experimentally without requiring a means of generating more exotic spin-squeezed states. The subject of the next section will delve a bit more deeply into possible experimental methods of performing a quantum non-demolition measure of atomic parity.

7 Quantum non-demolition measure of atomic parity

Here we will discuss several methods of performing a QND measure of atomic parity through the use of coupling between the atomic system with an ancillary subsystem. We begin by defining the even/odd atomic parity projection operators. That is, we define the operators that project the atomic state into even/odd numbers of excitations only. These are given by

$$\hat{\Pi}_{\mathrm{even}} = \sum_{m=-j}^{j} \cos^2\left[\frac{(j+m)\,\pi}{2}\right] |j,m\rangle\,\langle j,m|\,, \tag{42}$$

$$\hat{\Pi}_{\mathrm{odd}} = \sum_{m=-j}^{j} \sin^2\left[\frac{(j+m)\,\pi}{2}\right] |j,m\rangle\,\langle j,m|\,. \tag{43}$$

These projection operators satisfy the POVM condition $\sum_i \hat{\Pi}_i = \hat{I}$ and can be used to express the atomic parity operator by

$$\hat{\Pi} = \sum_i \lambda_i \hat{\Pi}_i = \hat{\Pi}_{\text{even}} - \hat{\Pi}_{\text{odd}}, \tag{44}$$

where λ_i are the eigenvalues of the parity operator, respectively. It can be shown, obviously, that

$$\langle \hat{\Pi}_{\text{even}} \rangle = \frac{1}{2}\left(1 + \langle \hat{\Pi} \rangle\right), \tag{45}$$

$$\langle \hat{\Pi}_{\text{odd}} \rangle = \frac{1}{2}\left(1 - \langle \hat{\Pi} \rangle\right), \tag{46}$$

where $\langle \hat{\Pi}_{\text{odd}} \rangle + \langle \hat{\Pi}_{\text{even}} \rangle = 1$. We note here that 'parity' is defined with respect to the number of atoms found in the excited state. That is, 'even' parity denotes an even number of atoms found in the excited state and 'odd' parity denotes and odd number of atoms found in the excited state. The same projection operators can be formed when defining parity with respect to the ground state. The two are related by $\langle \hat{\Pi}_{\text{excited}} \rangle = (-1)^{2j} \langle \hat{\Pi}_{\text{ground}} \rangle$. Next we introduce an ancillary atomic system $|\zeta, j_b\rangle_b$ as well as the coupling Hamiltonian and corresponding evolution operator:

$$\hat{H} = \hbar\chi \left(\hat{J}_0^a + \hat{J}_3^a\right)\left(\hat{J}_0^b + \hat{J}_3^b\right) \qquad \rightarrow \qquad \hat{U} = e^{-it\hat{H}/\hbar}, \tag{47}$$

where χ is the coupling strength. This interaction Hamiltonian is analogous to the field coupling cross-Kerr interaction. Presently, it is unknown whether this interaction has an atomic analogue. We define the initial state as

$$|\text{initial}\rangle = |\psi\rangle_a \otimes |\zeta, j_b\rangle = \sum_{m=-j_a}^{j_a} C_m^{(j_a)} |j_a, m\rangle_a \otimes \left(1 + |\zeta|^2\right)^{-j_b} \sum_{m'=-j_b}^{j_b} \binom{2j_b}{j_b + m'} \zeta^{j_b+m'} |j_b, m'\rangle_b . \tag{48}$$

Note that we wish to make a projective measurement on the ancillary atomic system (b-system) in order to determine the atomic parity of the target system (a-system). The final state is then

$$\begin{aligned} |\text{final}\rangle &= e^{-it\hat{H}/\hbar} |\text{initial}\rangle \\ &= \sum_{m=-j_a}^{j_a} C_m^{(j_a)} |j_a, m\rangle_a \otimes |\zeta e^{-it\chi(j_a+m)}, j_b\rangle . \end{aligned} \tag{49}$$

For the choice of $\chi t \rightarrow \pi$, this becomes

$$\begin{aligned} |\text{final}\rangle &= |\psi_{\text{even}}\rangle_a |\zeta, j_b\rangle_b + |\psi_{\text{odd}}\rangle_a |-\zeta, j_b\rangle_b \\ &= \sum_{m=-j_a}^{j_a} \left\{\cos^2\left[(j_a + m)\pi/2\right] |\zeta, j_b\rangle_b + \sin^2\left[(j_a + m)\pi/2\right] |-\zeta, j_b\rangle_b\right\} C_m^{(j_a)} |j_a, m\rangle \\ &= \sum_{m=-j_a}^{j_a} C_m^{(j_a)} |j_a, m\rangle_a |\Phi_m\rangle_b \end{aligned} \tag{50}$$

Now we look specifically at the ancillary atomic system, $|\Phi_m\rangle_b$. Obviously the system is entangled such that a projection onto the ancillary atomic system yielding the ACS characterized by parameter $-\zeta$ will project out odd atomic states in the target system and projection onto the ACS characterized by parameter $+\zeta$ will project out even atomic states in the target system. What we require is a means of determining which state the ancillary atomic system is in. Let's assume the ancillary atomic coherent is prepared such that $\zeta = -1$; this corresponds to a separable state in which all atoms of the ancillary atomic system are in the same superposition state

$$e^{-i\frac{\pi}{2}\hat{J}_2} |j, -j\rangle = |-1, j\rangle = |\psi_-\rangle^{\otimes N} = \frac{1}{2^{N/2}} \left(|g\rangle - |e\rangle\right)^{\otimes N} . \tag{51}$$

Similarly, we can also define the phase-rotated atomic coherent state

$$e^{-i\frac{\pi}{2}\hat{J}_2}\left|j,j\right\rangle = \left|1,j\right\rangle = \left|\psi_+\right\rangle^{\otimes N} = \frac{1}{2^{N/2}}\left(\left|g\right\rangle + \left|e\right\rangle\right)^{\otimes N}. \tag{52}$$

With this, we can rewrite the state $\left|\Phi_m\right\rangle_b$, assuming $\zeta = -1$, as

$$\begin{aligned}\left|\Phi_m\right\rangle_b &= \cos^2\left[\left(j_a+m\right)\pi/2\right]\left|-1,j_b\right\rangle_b + \sin^2\left[\left(j_a+m\right)\pi/2\right]\left|1,j_b\right\rangle_b \\ &= \cos^2\left[\left(j_a+m\right)\pi/2\right]e^{-i\frac{\pi}{2}\hat{J}_2^b}\left|j_b,-j_b\right\rangle_b + \sin^2\left[\left(j_a+m\right)\pi/2\right]e^{-i\frac{\pi}{2}\hat{J}_2^b}\left|j_b,j_b\right\rangle_b.\end{aligned} \tag{53}$$

Performing a single $\pi/2$-pulse yields the ancillary atomic system in the state

$$e^{i\frac{\pi}{2}\hat{J}_2^b}\left|\Phi_m\right\rangle_b = \cos^2\left[\left(j_a+m\right)\pi/2\right]\left|j_b,-j_b\right\rangle_b + \sin^2\left[\left(j_a+m\right)\pi/2\right]\left|j_b,j_b\right\rangle_b. \tag{54}$$

The final state of the ancillary atomic system is a superposition of all atoms in the exicted state and all atoms in the ground state. A measure of a single atom of the ancillary system is all that would be required in order to project the target atomic system into even/odd states. Note that this works for an arbitrary value of j_b; that means the ancillary atomic system can consist solely of a single atom. Next we will discuss a method involving a known coupling Hamiltonian.

Consider coupling to a field state. The interaction Hamiltonian is

$$\hat{H} = \hbar\chi\hat{b}^\dagger\hat{b}\hat{J}_3 \quad \rightarrow \quad \hat{U} = e^{-i\frac{t}{\hbar}\hat{H}}, \tag{55}$$

where $\{\hat{b},\,\hat{b}^\dagger\}$ are the usual boson annihilation and creation operators, respectively. Consider an ancillary field state, given by the usual coherent state

$$\left|\alpha\right\rangle_b = e^{-\frac{1}{2}\left|\alpha\right|^2}\sum_{n=0}^{\infty}\frac{\alpha^n}{\sqrt{n!}}\left|n\right\rangle_b. \tag{56}$$

The coupling Hamiltonian yields the final state

$$\left|\text{final}\right\rangle = \hat{U}\left|\text{initial}\right\rangle = \sum_{m=-j}^{j} C_m^{(j)}\left|j,m\right\rangle \otimes \left|\left(-1\right)^m\alpha\right\rangle_b. \tag{57}$$

This is a bit messier, as the final entangled state will depend greatly on the value of j. More specifically

$$\left|\text{final}\right\rangle = \begin{cases} \left|\psi_{\text{odd}}\right\rangle_a\left|-\alpha\right\rangle_b + \left|\psi_{\text{even}}\right\rangle_a\left|\alpha\right\rangle_b & j = 0,2,4..., \quad N = 0,4,8,... \\ \left|\psi_{\text{even}}\right\rangle_a\left|-\alpha\right\rangle_b + \left|\psi_{\text{odd}}\right\rangle_a\left|\alpha\right\rangle_b & j = 1,3,5..., \quad N = 2,6,10,... \\ \left|\psi_{\text{even}}\right\rangle_a\left|-i\alpha\right\rangle_b + \left|\psi_{\text{odd}}\right\rangle_a\left|i\alpha\right\rangle_b & j = \frac{1}{2},\frac{5}{2},\frac{9}{2}..., \quad N = 1,5,9,... \\ \left|\psi_{\text{odd}}\right\rangle_a\left|-i\alpha\right\rangle_b + \left|\psi_{\text{even}}\right\rangle_a\left|i\alpha\right\rangle_b & j = \frac{3}{2},\frac{7}{2},\frac{11}{2}..., \quad N = 3,7,11,... \end{cases} \tag{58}$$

In order for this procedure to be applicable, the total number of atoms involved must be known with certainty, as the resulting superposition state and subsequent detection scheme will greatly depend on having this information.

8 Signal-to-noise ratio: $\langle\hat{J}_z\rangle$ vs. $\langle\hat{\Pi}\rangle$ for the ACS and $\hat{J}_z$-op ACS

A useful metric for comparing the level of desired signal with the amount of background noise present is the signal-to-noise ratio (SNR). The SNR for an arbitrary detection observable $\hat{D}$ is given by

$$\text{SNR} = \frac{\langle\hat{D}\rangle}{\langle\left(\Delta\hat{D}\right)^2\rangle}. \tag{59}$$

We wish to compare the SNR when using parity-based detection as well as the when measuring the atomic inversion, while considering two different states: the atomic coherent state $\left|\zeta=-1,j\right\rangle$ and the $\hat{J}_z$-operated atomic coherent state $\left|\zeta=-1,j;1\right\rangle$. In terms of these detection observables, the respective SNRs simplify to

$$(\mathrm{SNR})_{\hat{J}_z} = \frac{\langle \hat{J}_z \rangle}{\sqrt{\langle \hat{J}_z^2 \rangle - \langle \hat{J}_z \rangle^2}} \tag{60}$$

$$(\mathrm{SNR})_{\hat{\Pi}} = \frac{\langle \hat{\Pi} \rangle}{\sqrt{1 - \langle \hat{\Pi} \rangle^2}}. \tag{61}$$

Note that the expectation values in Eqs.60 and 61 can be calculated for both states in question using the expressions found in Eqs.18 and 19 as well as Eqs.22 and 23. We plot $10\mathrm{Log}_{10}(SNR)$ against $N = 2j$, the total number of atoms in the system, in Fig.12 for both initial states.

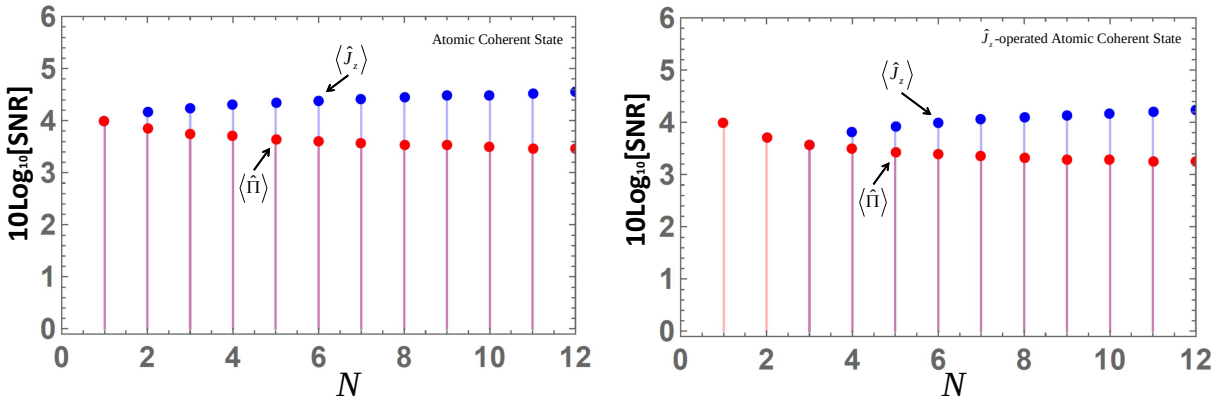

Figure 12: SNR in decibel scale plotted against total number of atoms $N = 2j$ for (a) an initial atomic coherent state and (b) an initial $\hat{J}_z$-operated atomic coherent state.

9 Measurement resolution for the $\hat{J}_z^2$-operated atomic coherent state

Next we consider a comparison of the resolution achieved when comparing parity-based detection and ground-state detection for the case of the $\hat{J}_z^2$-operated atomic coherent state as the state just prior to time evolution. Once again, the action of the Ramsey interferometer on the initial state $|\mathrm{in}\rangle = |j, -j\rangle$ is given by

$$\begin{aligned} |\Psi_{\mathrm{F}}\rangle &= e^{-i\frac{\pi}{2}\hat{J}_y} e^{-i\phi\hat{J}_z} \hat{J}_z^2 e^{-i\frac{\pi}{2}\hat{J}_y} |\mathrm{in}\rangle \\ &= e^{-i\frac{\pi}{2}\hat{J}_y} e^{-i\phi\hat{J}_z} |\zeta = -1, j; 2\rangle, \end{aligned} \tag{62}$$

where the state in the last line is given by

$$\begin{aligned} |\zeta = -1, j; 2\rangle &\propto \hat{J}_z^2 |\zeta = -1, j\rangle \\ &= \left[\frac{4^j j}{4}(3j-1)\right]^{-1/2} \sum_{m=-j}^{j} \binom{2j}{j+m}^{1/2} (-1)^{j+m} m^2 |j, m\rangle. \end{aligned} \tag{63}$$

Using Eq. 28, we can find the expectation value of the parity operator to be

$$\langle \hat{\Pi} \rangle_{\hat{J}_z^2\text{-op}} = \left[\frac{4^j j}{4}(3j-1)\right]^{-1} \sum_{m=-j}^{j} \binom{2j}{j+m} m^4 e^{-i2m\phi}, \tag{64}$$

and the expectation value of the ground-state projection operator

$$\langle \hat{P}_{-j}^{(j)} \rangle_{\hat{J}_z^2\text{-op}} = \left| \left[\frac{4^j j}{4}(3j-1)\right]^{-1/2} \sum_{m=-j}^{j} \binom{2j}{j+m}^{1/2} m^2 (-1)^{j+m} e^{i\phi m} d^j_{-j,m}\left(\tfrac{\pi}{2}\right) \right|^2. \tag{65}$$

Once again, unsurprisingly, we find a somewhat greater resolution for parity-based detection. Note that for both of these detection observables, one obtains greater resolution for larger numbers of atoms.

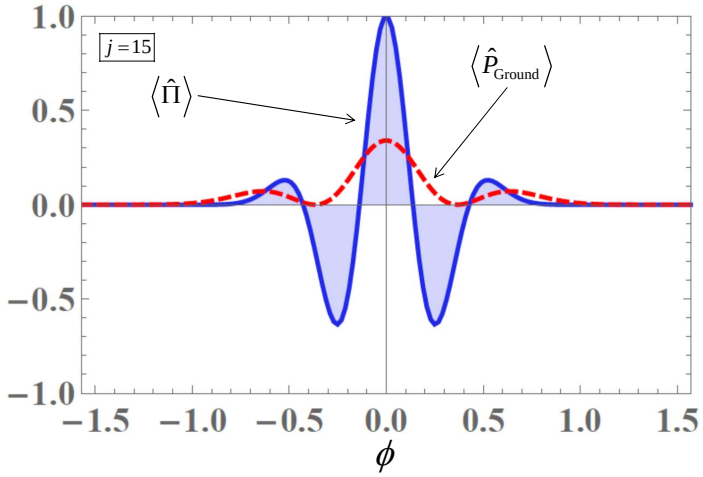

Figure 13: Ground state detection versus parity-based detection for an initial $\hat{J}_z^2$-operated atomic coherent state for $j = 15$.

10 Parity-based resolution using the $\hat{J}_z^q$-operated ACS for $q = 3, 4, 5$,...

Now we generalize to see the effect of increasing applications of $\hat{J}_z$ to the atomic coherent state. Note that increasing applications does not necessarily yield greater spin squeezing: for example, the $\hat{J}_z$-op ACS is more spin-squeezed than the $\hat{J}_z^2$-op ACS. Let's once again assume the state is initially prepared with all atoms in the ground state, that is $|\text{in}\rangle = |j, -j\rangle$. The action of the Ramsey interferometer is to transform an initial state $|\text{in}\rangle$ by

$$\begin{aligned} |\Psi_{\text{F}}\rangle &= e^{-i\frac{\pi}{2}\hat{J}_y} e^{-i\phi\hat{J}_z} e^{-i\frac{\pi}{2}\hat{J}_y} |\text{in}\rangle \\ &= e^{-i\frac{\pi}{2}\hat{J}_y} e^{-i\phi\hat{J}_z} |\zeta = -1, j\rangle \,, \end{aligned} \tag{66}$$

Let's consider the case where we act with the $\hat{J}_z^q$ operator after the first $\pi/2$-pulse, where $q = 2, 3, 4$. In this case the initial state is transformed by

$$\begin{aligned} |\Psi_{\text{F}}\rangle &= e^{-i\frac{\pi}{2}\hat{J}_y} e^{-i\phi\hat{J}_z} \hat{J}_z^q e^{-i\frac{\pi}{2}\hat{J}_y} |\text{in}\rangle \\ &= e^{-i\frac{\pi}{2}\hat{J}_y} e^{-i\phi\hat{J}_z} |\zeta = -1, j; q\rangle \,, \end{aligned} \tag{67}$$

where $|\zeta = -1, j; q\rangle \propto \hat{J}_z^q |\zeta = -1, j\rangle$, and where $|\zeta = -1, j\rangle$ is the atomic coherent state. We can calculate the expectation value of the parity operator at the output of the Ramsey interferometer for varying values of q to be

$$\langle\hat{\Pi}\rangle_{q=2} = \left(4^{j-1} j \left(3j-1\right)\right)^{-1} \sum_{m=-j}^{j} \binom{2j}{j+m} e^{2i\phi m} m^4 \tag{68}$$

$$\langle\hat{\Pi}\rangle_{q=3} = \left(2^{2j-3} j \left(15j^2 - 15j + 4\right)\right)^{-1} \sum_{m=-j}^{j} \binom{2j}{j+m} e^{2i\phi m} m^6 \tag{69}$$

$$\langle\hat{\Pi}\rangle_{q=4} = \left(4^{j-2} j \left(21j \left(5 \left(j-2\right) j + 7\right) - 34\right)\right)^{-1} \sum_{m=-j}^{j} \binom{2j}{j+m} e^{2i\phi m} m^8. \tag{70}$$

A plot of the expectation value of the parity operator versus the phase ϕ can be seen in Fig.14 for $q = 1, 2, 3, 4$. Not shockingly, we obtain greater resolution with successive actions of $\hat{J}_z$. Note that regardless of the number of times we act with the $\hat{J}_z$ operator, the expectation value of the parity operator has the form

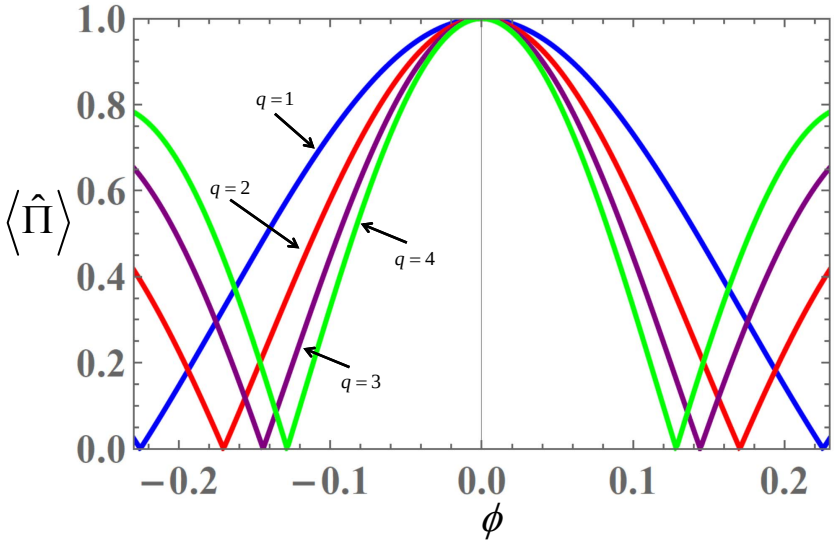

Figure 14: Parity-based resolution for the state $|\zeta = -1, j; q\rangle$ for $q = 1, 2, 3, 4$ for $N = 2j = 5$.

$$\langle\hat{\Pi}\rangle_q \propto \sum_{m=-j}^{j} \binom{2j}{j+m} e^{2i\phi m} m^{2q}, \tag{71}$$

where the constant of proportionality is related to the normalization factor of the initial state.

11 Parity-based resolution with arbitrary atomic coherent states generated after the first $\pi/2$-pulse

Once again, we assume a similar interferometer transformation, except now we assume the first λ-pulse generates an arbitrary atomic coherent state $|\zeta, j\rangle$

$$\begin{aligned} |\Psi_{\mathrm{F}}\rangle &= e^{-i\frac{\pi}{2}\hat{J}_y} e^{-i\phi\hat{J}_z} e^{-i\lambda\hat{O}} |\mathrm{in}\rangle \\ &= e^{-i\frac{\pi}{2}\hat{J}_y} e^{-i\phi\hat{J}_z} |\zeta, j\rangle , \end{aligned} \tag{72}$$

where $\hat{O}$ is the operator driving the evolution of the initial state. This operator is well known in the literature. The output state is given by

$$\begin{aligned} |\Psi_{\mathrm{F}}\rangle &= \left(1 + |\zeta|^2\right)^{-j} \sum_{m=-j}^{j} \sum_{m'=-j}^{j} \binom{2j}{j+m}^{1/2} \zeta^{j+m} e^{-i\phi m} d^j_{m',m}\left(\tfrac{\pi}{2}\right) |j, m'\rangle \\ &= \sum_{m'=-j}^{j} B_{j,m'}(\zeta, \phi) |j, m'\rangle . \end{aligned} \tag{73}$$

Note that in Eq. 72 and 73, the parameter ζ is given in terms of angles relative to the Bloch sphere by $\zeta = e^{i\sigma} \tan\frac{\theta}{2}$, where $0 \leq \sigma \leq 2\pi$ and $0 \leq \theta \leq \pi$. The expectation value of the parity operator is then simply

$$\langle\hat{\Pi}\rangle = \langle\Psi_{\mathrm{F}}| e^{i\pi\left(j - \hat{J}_z\right)} |\Psi_{\mathrm{F}}\rangle = \sum_{m'=-j}^{j} \left|B_{j,m'}(\zeta, \phi)\right|^2 e^{i\pi\left(j - m'\right)}. \tag{74}$$

We are interested in plotting this versus the phase angle ϕ and the state angle θ, in a three-dimensional plot for set values of j and σ. The goal is to see whether the angle associated with the initial atomic coherent state affects measurement resolution at the output; or if it simply shifts the peak from $\phi = 0$.

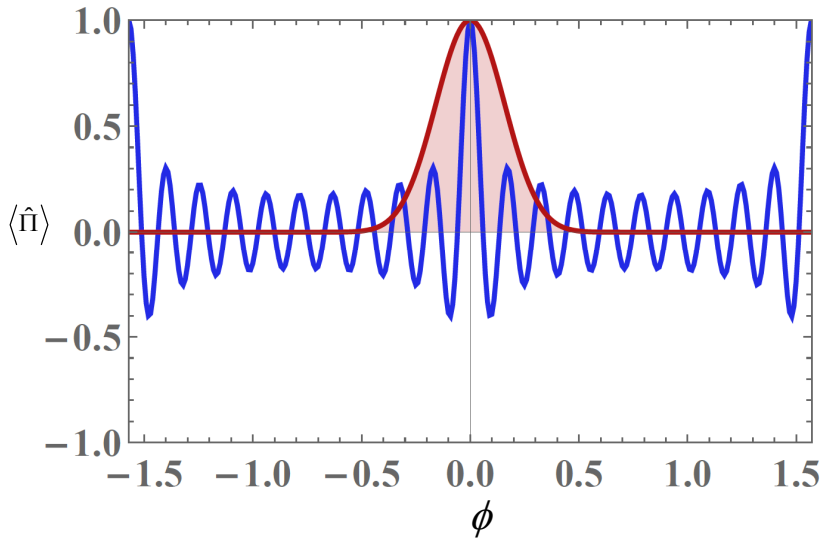

Figure 15: Parity-based resolution for $M = 0$ and $j = 20$ (blue). For reference, a plot of the ACS, $M = -j$, for the same value of j is superposed onto the plot (red).

12 Parity-based resolution for an arbitrary initial superposition state

We assume the interferometer transforms the initial state in a similar fashion as the earlier work, however now we assume the initial state to be some arbitrary superposition of atomic states, rather than assuming all atoms are initially prepared in the ground state. That case would yield the atomic coherent state with $\zeta = -1$ after the first $\pi/2$-pulse. The output state is given by

$$\begin{aligned} |\Psi_{\rm F}\rangle &= e^{-i\frac{\pi}{2}\hat{J}_y} e^{-i\phi\hat{J}_z} e^{-i\frac{\pi}{2}\hat{J}_y} |j, M\rangle \\ &= e^{-i\frac{\pi}{2}\hat{J}_y} e^{-i\phi\hat{J}_z} \times \sum_{m=-j}^{j} d^j_{m,M}\left(\tfrac{\pi}{2}\right) |j, m\rangle \\ &= \sum_{m'=-j}^{j} A^j_{m'}\left(\phi|M\right) |j, m'\rangle\,, \end{aligned} \tag{75}$$

where once again $d^j_{m',m}(\beta)$ are the usual Wigner-d matrix elements given by $\langle j, m'|e^{-i\beta\hat{J}_y}|j, m\rangle$ and the coefficients in the last line of Eq. 75 are given by

$$A^j_{m'}\left(\phi|M\right) = \sum_{m=-j}^{j} d^j_{m,M}\left(\tfrac{\pi}{2}\right) d^j_{m',m}\left(\tfrac{\pi}{2}\right) e^{-i\phi m}. \tag{76}$$

The expectation value of the parity operator is then given by

$$\langle\hat{\Pi}\rangle = \sum_{m'=-j}^{j} \left|A^j_{m'}\left(\phi|M\right)\right|^2 e^{i\pi\left(j-m'\right)}. \tag{77}$$

Note that for the selection $M = -j$, we should recover the well known result

$$\langle\hat{\Pi}\rangle\Big|_{M=-j} = \cos^{2j}\left(\phi\right). \tag{78}$$

We plot the expectation value of the parity operator $\langle\hat{\Pi}\rangle$ versus the phase ϕ in Fig.15 for $j = 20$ and $M = 0$. Note that for $M = 0$, we must have integer values of j; or even numbers of atoms only. Note that while the expectation value of the parity operator is more oscillatory, it *is* narrower at the peak than the case in which all atoms are initially in the ground state.

13 Wigner function for atomic ensembles of two-level atoms

Here we discuss, for pedagogical interest, how one would define the Wigner function for an arbitrary atomic state in terms of the multipole operator $\hat{T}_{K,Q}$. A general atomic state, written in terms of the Dicke states $|j,m\rangle$, is given by

$$|\psi\rangle = \sum_{m=-j}^{j} C_m^{(j)} |j,m\rangle \,. \tag{79}$$

The Wigner function can be written as

$$W(\theta,\phi) = \sqrt{\frac{2j+1}{4\pi}} \sum_{K=0,1,..}^{2j} \sum_{Q=-K}^{K} \langle \hat{T}_{K,Q}^{\dagger} \rangle \, Y_Q^K(\theta,\phi) \,, \tag{80}$$

where $Y_Q^K(\theta,\phi)$ are the usual spherical harmonics. The Wigner function of Eq. 80 should satisfy the normalization condition

$$\int_0^{\pi} \int_0^{2\pi} W(\theta,\phi) \sin\theta \, d\theta d\phi = 1. \tag{81}$$

The Hermitian conjugate $\hat{T}_{K,Q}^{\dagger}$ can be written in terms of the multipole operator $\hat{T}_{K,Q}$ by

$$\begin{aligned} \hat{T}_{K,Q}^{\dagger} &= (-1)^Q \hat{T}_{K,-Q} \\ &= (-1)^Q \sum_{p=-j}^{j} \sum_{p'=-j}^{j} (-1)^{j-p} \sqrt{2K+1} \begin{pmatrix} j & K & j \\ -p & -Q & p' \end{pmatrix} |j,p\rangle \langle j,p'| \,, \end{aligned} \tag{82}$$

where the matrix appearing in Eq. 82 are the Wigner-3j symbol.

14 Post-interferometer entanglement between $N = 2j = 3$ atoms

We investigate the entanglement between individual atomic states after the interferometer. To that end, we consider the linear entropy, which is simply the linear first order approximation of the von Neumann entropy. It is essentially a measure of how mixed a reduced density operator is. Consider the state after the interferometer

$$\begin{aligned} |\Psi_{\rm F}\rangle &= e^{-i\frac{\pi}{2}\hat{J}_y} e^{-i\phi\hat{J}_z} \hat{J}_z^Q e^{-i\frac{\pi}{2}\hat{J}_y} |j,-j\rangle \\ &= e^{-i\frac{\pi}{2}\hat{J}_y} e^{-i\phi\hat{J}_z} |\zeta=-1,j;Q\rangle \,, \end{aligned} \tag{83}$$

where the state in the last line of Eq. 83 is the $\hat{J}_z^Q$-operated atomic coherent state, given by

$$\begin{aligned} |\zeta=-1,j;Q\rangle &= \eta_j^{(Q)} \sum_{m=-j}^{j} \binom{2j}{j+m}^{1/2} (-1)^{j+m} \, m^Q \, |j,m\rangle \,, \\ &= \eta_j^{(Q)} \sum_{m=-j}^{j} \Lambda_{j,m}^{(Q)} |j,m\rangle \end{aligned} \tag{84}$$

where $\eta_j^{(Q)}$ is determined by normalization. The output state then has the form

$$|\Psi_{\rm F}\rangle = \sum_{m'=-j}^{j} \Gamma_{j,m'}^{(Q)}(\phi) \, |j,m'\rangle \,, \tag{85}$$

where the new coefficients are given by

$$\Gamma_{j,m'}^{(Q)}(\phi) = \eta_j^{(Q)} \sum_{m=-j}^{j} \Lambda_{j,m}^{(Q)} e^{-i\phi m} d_{m',m}^{j}\left(\tfrac{\pi}{2}\right). \tag{86}$$

Once again, the Wigner-d matrix elements, $d^{j}_{m',m}(\beta)$ is given previously in the text. Setting $j = 3/2$, that is, three atoms present, and tracing out two of the atoms, we find the reduced density operator

$$\hat{\rho}_{\text{out},a} = \Omega_{gg}|g\rangle\langle g| + \Omega_{eg}|e\rangle\langle g| + \Omega_{ge}|g\rangle\langle e| + \Omega_{ee}|e\rangle\langle e|, \tag{87}$$

where, dropping some sub- and super-scripts for notational convenience

$$\begin{aligned}
\Omega_{gg} &= |\Gamma_{-3/2}|^2 + \tfrac{1}{3}|\Gamma_{1/2}|^2 + \tfrac{2}{3}|\Gamma_{-1/2}|^2 \\
\Omega_{ee} &= |\Gamma_{3/2}|^2 + \tfrac{1}{3}|\Gamma_{-1/2}|^2 + \tfrac{2}{3}|\Gamma_{1/2}|^2 \\
\Omega_{eg} &= \tfrac{1}{\sqrt{3}}\Gamma_{-1/2}\Gamma^*_{-3/2} + \tfrac{1}{\sqrt{3}}\Gamma_{3/2}\Gamma^*_{-1/2} + \tfrac{2}{3}\Gamma_{1/2}\Gamma^*_{-1/2} \\
\Omega_{ge} &= \tfrac{1}{\sqrt{3}}\Gamma_{-3/2}\Gamma^*_{-1/2} + \tfrac{1}{\sqrt{3}}\Gamma_{1/2}\Gamma^*_{3/2} + \tfrac{2}{3}\Gamma_{-1/2}\Gamma^*_{1/2}.
\end{aligned} \tag{88}$$

Squaring the density operator yields

$$\hat{\rho}^2_{\text{out},a} = \begin{pmatrix} \Omega^2_{gg} + \Omega_{ge}\Omega_{eg} & \Omega_{eg}(\Omega_{ee} + \Omega_{gg}) \\ \Omega_{ge}(\Omega_{ee} + \Omega_{gg}) & \Omega^2_{ee} + \Omega_{ge}\Omega_{eg} \end{pmatrix}, \tag{89}$$

and the purity of the state is given by the usual $P = \text{Tr}[\hat{\rho}_{\text{out},a}]$ and the linear entropy is then

$$S_{\text{Lin}} = 1 - P. \tag{90}$$

This state has been shown to be more entangled for increasing values of Q, however the degree of spin squeezing does *not* necessarily increase with increasing values of Q. In fact, the $Q = 1$ state is less entangled but more spin-squeezed than the $Q = 2$.

15 Conclusion

We have shown that atomic parity $\hat{\Pi} = \text{Exp}\left[i\pi\left(\hat{J}_0 + \hat{J}_3\right)\right]$ provides a substantial increase in measurement resolution when used as a detection observable in multi-atom Ramsey interferometry. In addition to this, we have demonstrated that the enhancement of measurement resolution increases with larger numbers of atoms in the ensemble. This was done in the context of an initial atomic coherent state, the spin-squeezed $\hat{J}_z$-operated atomic coherent state and the more general $\hat{J}^q_z$-operated atomic coherent state. Furthermore, we considered several other means of measurement including projection onto the balanced $|j, 0\rangle$, valid for integer values of j. In this particular case, when scaled to unity, the measurement resolution agrees with that of atomic parity.

We go on to also discuss a plausible quantum non-demolition means of implementing measurement of atomic parity using the atomic analogue of field cross-Kerr interations by coupling the atomic system with an ancillary system of arbitrary size. An alternative means of parity measurement can be shown through the use of a well known atom-field coupling Hamiltonian. In this case, however, the number of atoms must be known with certainty.